Progress of Theoretical Physics, Vol. 53, No. 1, January 1975

Application of Mode-Coupling Theory to Nonlinear Stress Tensor in Fluids

Tomoji YAMADA and Kyozi KAWASAKI*

Department of Applied Science, Kyushu University, Fukuoka 812
**Research Institute for Fundamental Physics, Kyoto University*
Kyoto 606

(Received July 3, 1974)

In a steady state of fluid the nonlinear dependence of stress tensor on a thermal driving force is investigated by a direct extension of the mode-coupling theory to far-from-equilibrium situation. The steady state is generated from a local equilibrium state having the same average values of gross variables as in the steady state. In the lowest approximation for the mode-coupling term the explicit expression of the stress tensor is obtained and evaluated. The effects of the higher mode-coupling approximations on the stress tensor are also briefly examined.

§ 1. Introduction

Recently the nonlinear stress tensor in a classical fluid was studied by Kawasaki and Gunton[1] (herafter referred to as KG). They started with the Liouville equation and made use of the projection operator to obtain the stress tensor. In the present paper we examine the same problem by a direct extension of the mode-coupling theory[2a] to far-from-equilibrium situation. This approach makes it feasible to develop a systematic approximation scheme in terms of the mode-coupling theory. Both in KG and in the present work a linearized hydrodynamic approximation is adopted in the calculation of the stress tensor. The justification of this approximation can be more easily examined by the present work than by former.[1]

The derivation of the steady state distribution is based on the fact that the difference between the local equilibrium distribution and the true distribution functions quickly disappears after a time which is larger than the periods of the microscopic fluctuations but shorter than the time scale of the variation of the macroscopic variables. A formulation of this problem is found in Ref. 3). The most interesting feature in the nonlinear transport is the existence of nonanalytic terms in the transport coefficients with respect to a thermal driving force.[1),4)] These nonanalytic terms arise because of the presence of a diffusion mode. The diffusion mode brings the so-called long-time tail into various time correlation functions.[5)]

In § 2 we derive expressions for the nonlinear stress tensor in a steady state with a shear velocity gradient. In the lowest approximation for the mode-

coupling term an expression for the stress tensor is obtained. This approximation is basically the same as that which was used by Zaitsev and Shliomis[6] to study fluctuations near the convective instability. Section 3 is devoted to discussion and higher-order approximations are examined.

§ 2. Steady state distribution and nonlinear stress tensor

We start with the Fokker-Planck equation corresponding to the nonlinear Langevin equation:[2]

$$\frac{\partial}{\partial t}P(a,t)=H(a)P(a,t), \tag{1}$$

where $P(a,t)$ is the probability distribution function for gross variables. The operator H is

$$H(a)=\sum_i L_i^0\frac{\partial^2}{\partial a_i\partial a_{i*}}-\sum_i\frac{\partial}{\partial a_i}[v_i(a)+L_i^0F_{i*}(a)]. \tag{2}$$

The bare Onsager kinetic coefficients L_i^0 are assumed to be independent of the gross variables. We further assume that the probability distribution takes the Gaussian form in both equilibrium and local equilibrium states in the following way: For equilibrium state,

$$P_e(a)=\text{const}\times\exp[-\tfrac{1}{2}\sum_i|a_i-\langle a_i\rangle_e|^2] \tag{3}$$

and for local equilibrium state,

$$P_l(a)=\text{const}\times\exp[-\tfrac{1}{2}\sum_i|a_i-\langle a_i\rangle_l|^2], \tag{4}$$

where $\langle a_i\rangle_e$ and $\langle a_i\rangle_l$ are the averages of a_i in equilibrium and local equilibrium states, respectively. In effect we are assuming that $P_l(a)$ is a displaced Gaussian since the local equilibrium distribution can be constructed by multiplying the factor $\exp[-\sum_i b_ia_i]$ to $P_e(a)$, where $\{b_i\}$ are the fields conjugate to $\{a_i\}$.[3]

We then find

$$F_j(a)=-a_{j*}' \tag{5}$$

and

$$v_i(a)=i\omega_ia_i'-i\sum_{j,l}\mathcal{V}_{ijl}[a_j'a_l'-\delta_{jl*}] \tag{6}$$

with

$$a_i'\equiv a_i-\langle a_i\rangle_e.$$

Let us now suppose that the system is in a local equilibrium state at $t=0$. For $t>0$, $P(a,t)$ will deviate from P_l by virtue of its time evolution, Eq. (1). The function $P(a,t)$ will reach an approximate steady state P_s after a time τ which is longer compared with the periods of oscillations of fluctuations of $\{a\}$ but is shorter compared with the macroscopic time when the averages $\langle a_i\rangle$ change

appreciably. This fact is expressed as

$$P_s(a) \simeq e^{\tau H} P_l(a) = P_l(a) + \int_0^\tau dt\, e^{tH} H P_l\,. \tag{7}$$

The steps leading to Eq. (7) can be made formally more precise by employing a projection operator technique as was done by one of the authors (K.K.).[5] Only the results are quoted here.

By introducing a projection operator $\mathcal{P}$ which acts on an arbitrary function $F(a)$ as

$$\mathcal{P}F(a) = \int da' \left[1 - \sum_i \frac{\partial}{\partial a_i}(a_i' - \langle a_i \rangle_l)\right] F(a') P_l(a), \tag{8}$$

P_s can be rewritten as

$$P_s(a) = \left\{1 + \int_0^\infty dt\, e^{t\mathcal{Q}H} \mathcal{Q} H\right\} P_l(a) \tag{9}$$

with $\mathcal{Q} \equiv 1 - \mathcal{P}$. The details are given in Ref. 3).

We can transform HP_l as follows:

$$H(a)P_l(a) = [H(a) - H(a-c)]P_l(a) = [H_1(a) + H'(a)]P_l(a) \tag{10}$$

with

$$c_i \equiv \langle a_i \rangle_l - \langle a_i \rangle_e\,,$$

where

$$H_1(a) \equiv -\sum_i \frac{\partial}{\partial a_i} K_i(c) \tag{11}$$

with

$$K_i(c) \equiv v_i(c) - L_i^0 c_i$$

and

$$H'(a) \equiv 2i \sum_{i,j,l} \frac{\partial}{\partial a_i} \mathcal{V}_{ijl} c_j (a_l - \langle a_l \rangle_l), \tag{12}$$

where use has been made of the facts that $H(a)P_e(a) = 0$ and $P_l(a) = P_e(a-c)$. From now on we choose $\langle a_i \rangle_l = 0$.

By noting that

$$\mathcal{Q} H_1 P_l(a) = 0 \tag{13}$$

and

$$\mathcal{Q} H' P_l(a) = O P_l \tag{14}$$

with

$$O \equiv -2i \sum_{i,j,l} \mathcal{V}_{ijl} (a_i^* a_l - \langle a_i^* a_l \rangle_l) c_j$$

$$=i\sum_{i,j,l} {}^{C}V_{j*il}(a_i a_l - \langle a_i a_l\rangle_l)c_j\,, \tag{15}$$*)

the steady-state average $\langle X\rangle_s$ of an arbitrary function of $\{a\}$ can be obtained as

$$\langle X\rangle_s = \langle X\rangle_l + \int_0^\infty dt \langle O[\exp t\tilde{Q}\tilde{H}]\tilde{Q}X(a)\rangle_l\,, \tag{16}$$

where $\tilde{H}$ is the adjoint operator of H:

$$\tilde{H} = \tilde{H}_1 + \tilde{H}_L + \tilde{H}_v\,, \tag{17}$$

$$\tilde{H}_1 = \sum_i K_i(c)\frac{\partial}{\partial a_i}\,, \tag{18}$$

$$\tilde{H}_L = \sum_i L_i{}^0 \frac{\partial^2}{\partial a_i \partial a_{i*}} + \sum_{i,j}{}' [i\tilde{\omega}_{ij} - L_i{}^0\delta_{ij}]a_j \frac{\partial}{\partial a_i}\,, \tag{19}$$

$$\tilde{H}_v = \sum_i v_i(a)\frac{\partial}{\partial a_i} \tag{20}$$

with

$$\tilde{\omega}_{ij} \equiv \omega_i \delta_{ij} + 2\sum_l {}^{C}V_{ijl}c_l\,.$$

Here we have defined another projection operator $\tilde{Q} \equiv 1 - \tilde{\mathcal{P}}$, where $\tilde{\mathcal{P}}$ is a projection operator which acts on an arbitrary function of $\{a\}$ as

$$\tilde{\mathcal{P}}G(a) = \langle G\rangle_l + \sum_i \langle a_{i*}G(a)\rangle_l a_i\,. \tag{21}$$

Linearized approximation

Now, we examine Eq. (16) by discarding $\tilde{H}_v$ in Eq. (17). This linearization is made in the same spirit as the use of linearized hydrodynamics in evaluating transport coefficients by the mode-coupling theory, and hence it should not be affected by the fact that we are interested in nonlinear transport, which is taken care of by our use of local equilibrium state arbitrarily far from equilibrium. Effects of $\tilde{H}_v$ will be considered in the next section and in Appendix C.

Let us now consider the following form of an operator X:

$$X(a) = a_i a_j - \langle a_i a_j\rangle_l\,. \tag{22}$$

As will be shown in Appendix A, Eq. (16) becomes

$$\langle X(a)\rangle_s = \int_0^\infty dt \langle O a_i(t) a_j(t)\rangle_l dt\,, \tag{23}$$

where

$$a_i(t) = [\exp(tM)a]_i \tag{24}$$

with

*) In order to derive Eq. (15) we have used the relations

$$\langle a_i a_{j*}\rangle_l = \delta_{ij} \text{ and } {}^{C}V_{ijl} + {}^{C}V_{j*i*l} + {}^{C}V_{i*l*j} = 0\,.$$

$$M_{ij} \equiv i\tilde{\omega}_{ij} - L_i^0 \delta_{ij} . \tag{25}$$

Stress tensor

We now apply this formalism to the evaluation of stress tensor P^* (more precisely, the contribution of long-wavelength transverse velocity fluctuations to P^*) which is given by KG (3·24) and (3·26)

$$P^* = \langle J^* \rangle_s . \tag{26}$$

According to KG, we put

$$J^* = k_B T \sum_k (\boldsymbol{u}_k \boldsymbol{u}_{k^*} - \langle \boldsymbol{u}_k \boldsymbol{u}_{k^*} \rangle_i), \tag{27}$$

where $\boldsymbol{u}_k$ is the dimensionless transverse velocity fluctuation which consists of two independent components perpendicular to a wave vector $\boldsymbol{k}$. Each component is normalized in such a way that its equilibrium average square fluctuation reduces to unity.

We choose $\{a\}$ to be a set of the local velocity $\boldsymbol{u}_k$. The average local velocity in the dimensionless unit is given by

$$u_x = 0, \quad u_y = D\sqrt{\rho/k_B T}\, x, \quad u_z = 0, \tag{28}$$

where ρ and T denote the mass density and the temperature, respectively. Inserting the expression*)

$$\mathcal{V}_{\boldsymbol{q}\alpha, \boldsymbol{k}\beta, \boldsymbol{q}-\boldsymbol{k}\tau} = \sqrt{\frac{k_B T}{\rho}} \left[\frac{1}{2} (q_\beta \delta_{\alpha\tau} + q_\tau \delta_{\alpha\beta}) - \frac{q_\alpha q_\beta q_\tau}{q^2} \right] \tag{29}$$

into Eq. (15), we find

$$O = -\frac{D}{V} \sum_k [u_k{}^x u_{-k}^y - \langle u_k{}^x u_{-k}^y \rangle_i]. \tag{30}$$

Then, we obtain

$$P_{\alpha\beta}^* = -\frac{k_B T D}{V} \sum_k \sum_{k'} \int_0^\infty \langle u_{k'}^x u_{-k'}^y u_k{}^\alpha(t)\, u_{-k}^\beta(t) \rangle_{ic} dt , \tag{31}$$

where the subscript c means that the cumulant average is taken by regarding each pair $u_k{}^\alpha u_{-k}^\beta$ as a single unit. The replacement of the bare Onsager kinetic coefficient L_i^0 by $(\eta/\rho)k^2$ and the use of Eqs. (24) and (25) yield the linearized hydrodynamic equation

$$\frac{d}{dt} u_k{}^\alpha(t) = -\frac{\eta}{\rho} k^2 u_k{}^\alpha(t) + D\left(k_y \frac{\partial}{\partial k_x} u_k{}^\alpha(t) + \frac{2k_y k_\alpha}{k^2} u_k{}^x(t) - \delta_{\alpha y} u_k{}^x(t) \right). \tag{32}$$

This equation-of-motion is equivalent to KG (4·6) except that the latter is time reversed. The use of Eq. (32) enables evaluation of the stress tensor, Eq. (31). This is done in Appendix B. By defining the nonlinear shear viscosity as

*) In the actual calculation instead of dealing with two components of $\boldsymbol{u}_k$ we work with three components u_k^α, $\alpha = x, y, z$.[2a]

$$\eta(D) \equiv -P_{xy}^*/D\,, \tag{33}$$

the results are

$$\begin{aligned}
\Delta\eta &\equiv \eta(D) - \eta(0) = C_0 k_B T (\rho/\eta)^{3/2} D^{1/2}\,,\\
\Delta_x &\equiv P_{xx}^*(D) - P_{xx}^*(0) = C_1 k_B T (\rho D/\eta)^{3/2}\,,\\
\Delta_y &\equiv P_{yy}^*(D) - P_{yy}^*(0) = C_2 k_B T (\rho D/\eta)^{3/2}\,,\\
\Delta_z &\equiv P_{zz}^*(D) - P_{zz}^*(0) = C_3 k_B T (\rho D/\eta)^{3/2}\,,
\end{aligned} \tag{34}$$

where the numerical coefficients C_0, C_1, C_2 and C_3 are $-3.0_5\times10^{-3}$, $1.0_6\times10^{-2}$, $4.2_8\times10^{-2}$ and $5.6_7\times10^{-3}$, respectively. These numbers are to be compared with -5.1×10^{-3}, -1.7×10^{-3}, 5.0×10^{-3} and -4.6×10^{-3} given in KG, respectively. The difference between these numerical values and those in KG is caused by two reasons: (A) In the latter the time correlation functions of the quantities $u_{k'}^x(-t)u_{-k'}^y(-t)$ and $u_k^\alpha u_{-k}^\beta$ enter into the expression of stress tensor, where $u_{k'}^x(-t)$ obeys the time reversed form of Eq. (32); (B) the higher order current correlation functions are included in KG. In terms of mode-coupling theory the higher order current correlation functions which come from a different origin from that of KG appear if the mode-coupling operator $\tilde{H}_v$ is taken into account. This problem will be examined in the next section. Note that this circumstance also explains the small numerical difference between the results of Fixman and Botch[7] and those of Yamada and Kawasaki[5] for nonlinear shear viscosity of binary fluids near the critical point.

§ 3. Discussion

In the preceding section and Appendix B we obtain the stress tensor in the lowest approximation to the mode-coupling operator $\tilde{H}_v$. In this section we briefly consider the effect of the higher order correction of the operator $\tilde{H}_v$. Since we are only interested in the D-dependence of the quantities

$$S_{\alpha\beta} \equiv \int_0^\infty dt \langle J_{xy}^* [\exp t\tilde{Q}\tilde{H}]\tilde{Q}J_{\alpha\beta}^*\rangle_t\,, \tag{35}$$

we take the following Fokker-Planck operator $\tilde{H}$:

$$\tilde{H} = \tilde{H}_0 + \tilde{H}_v \tag{36}$$

with

$$\tilde{H}_0 = \sum_i{}' L_i^0 \frac{\partial^2}{\partial a_i \partial a_{i^*}} + \sum_i{}' [i\omega_i - L_i^0] a_i \frac{\partial}{\partial a_i}\,, \tag{37}$$

$$\tilde{H}_v = \sum_i{}' v_i(a) \frac{\partial}{\partial a_i}\,, \tag{38}$$

where the summation $\sum'$ means that the magnitude of wave number is limited above a certain cutoff k_0 which is proportional to $(\rho D/\eta)^{1/2}$. Since Eq. (36) is

Fig. 1. The lowest order diagram for the nonlinear correction.

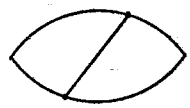

Fig. 2. The next lowest order diagram.

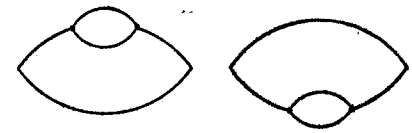

Fig. 3. Diagrams which renormalize propagators.

of the same form as was used in mode-coupling theory[2a] except for the existence of the lower cutoff, we can use much of the techniques and the terminologies in Ref. 2a) to estimate the quantities $S_{\alpha\beta}$. The lowest and the next lowest diagrams with respect to the mode-coupling operator $\tilde{H}_v$ are shown in Figs. 1 $\sim$3 where the time increases from the right to the left and a free propagator

$$G_j^0(t) \equiv \exp[(i\omega_j - L_j^0)t], \quad t>0, \qquad =0, \quad t<0 \tag{39}$$

is represented by a solid line and we find that a disconnected diagram and a diagram which is connected by a single line do not appear due to the existence of the projection operator $\tilde{Q}$.[3),*] Contributions from Fig. 3 serve to renormalize a free propagator and to replace the bare Onsager kinetic coefficient by the renormalized one. Therefore, hereafter we only deal with diagrams which do not contain self-energy corrections such as one shown in Fig. 3, and replace the free propagators in Figs. 1 and 2 by the renormalized ones in which the renormalized viscosity $\eta(D)$ is substituted for the bare one η. In higher order diagrams the same replacement is made. Since the evaluation of Fig. 1 has already been carried out in the preceding section, we here concentrate on the estimate of the contributions from Fig. 2. By omitting the numerical coefficients the contributions from Fig. 2 approximately become

$$S_{\alpha\beta} \sim \frac{1}{V^2} \sum_{\boldsymbol{k},\boldsymbol{k}'}{}' \frac{1}{k^2} k \frac{1}{k^2 + (\boldsymbol{k}-\boldsymbol{k}')^2 + k'^2} k' \frac{1}{k^2}$$
$$\sim \text{const} + O[k_0^2 \ln(k_M/k_0)], \tag{40}$$

where the magnitude of all internal momenta $\boldsymbol{k}$, $\boldsymbol{k}'$ and $(\boldsymbol{k}-\boldsymbol{k}')$ has the upper and lower cutoff wave numbers k_M and k_0, respectively. If the lower limit k_0 is put equal to zero (namely, put $D=0$) the constants in S_{xx}, S_{yy} and S_{zz} vanish due to symmetry. Comparing Eq. (34) with (35) we conclude that the singular correction to stress tensor from Fig. 2 is smaller than that from Fig. 1. It is

*) This can be proved by the second quantization technique.[3)]

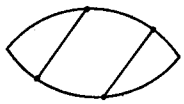

Fig. 4. A higher order diagram.

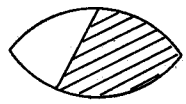

Fig. 5. A type of diagram which is of $O(k_0^2)$ at most.

difficult to estimate the higher order diagrams than that in Fig. 2. However, the study of the diagram in Fig. 4 shows that the contribution of this diagram has a form const$+O[k_0^2 k_M]$. Then we can deduce from this result and Eq. (40) that a $(2n)$-vertex diagram has a contribution to $S_{\alpha\beta}$ of the form const$+O[k_0^2 k_M^{(n-1)}]$ for $n \geq 1$.*) The second term arises, for example, from a diagram shown in Fig. 5. The shaded area consists of propagators, the magnitude of whose internal momenta is of $O(k_M)$ and the left two solid lines have internal momenta of $O(k_0)$. Thus, if this deduction is true, it is sufficient to consider the diagram in Fig. 1 in order to evaluate the dominant nonlinear correction to the stress tensors. Since a renormalized propagator is used in the above consideration, $\eta(D)$ has a general form

$$\eta(D) = F(\eta(D)) + C_0 k_B T (\rho/\eta)^{3/2} D^{1/2}. \tag{41}$$

Then we have a self-consistent equation for determining the $\eta(D)$. Therefore the numerical coefficient C_0 above is replaced by another one multiplied by a factor $O(1)$. However, this fact means that the modes having large wave numbers necessarily participate in the present consideration. The determination of the precise value of C_0 is, however, beyond the scope of the present paper.

Recently Ashurst and Hoover[8] reported the molecular dynamics results of the nonlinear shear viscosity $\Delta\eta$. Their $\Delta\eta$ seems to be consistent with $D^{1/2}$-dependence but the coefficient C_0 is rather too small to account for their results. We conclude that their $\Delta\eta$ is probably due to more microscopic processes explained by the Eyring formula.[9] In order to see the effects predicted by KG, one may have to see $\Delta\eta$ very precisely for much smaller values of D than those of Ashurst and Hoover.

Acknowledgement

The authors would like to thank Professor J. D. Gunton for informing us of the details of the computer program used in KG.

*) This may be proved by increasing the number n step by step from 1 and assigning factors k^3, k and k^{-2} to an integral of the internal momenta of the diagram, a vertex and a time integral at the intermediate state, respectively, where k is either k_0 or k_M. This procedure can be easily done up to $n=2$ but becomes hard as n increases. This problem will be further investigated in Appendix C.

Appendix A

Using an abbreviated notation

$$A_{ij} \equiv a_i a_j - \langle a_i a_j \rangle_l \,, \tag{A·1}$$

we first find that

$$(1-\tilde{\mathcal{P}})\tilde{H}_1 A_{ij} = (1-\tilde{\mathcal{P}})\,(K_i(c)a_j + K_j(c)a_i) = 0\,. \tag{A·2}$$

$\tilde{H}_1$ in Eq. (16) can be thus dropped. Next we obtain

$$(1-\tilde{\mathcal{P}})\tilde{H}_L A_{ij} = \sum_l (M_{jl}A_{li} + M_{il}A_{lj}) \tag{A·3}$$

with

$$M_{ij} \equiv i\tilde{\omega}_{ij} - L_i^0 \delta_{ij}\,.$$

Repeating the same operation on A_{ij}, we have

$$[(1-\tilde{\mathcal{P}})\tilde{H}_L]^n A_{ij} = \sum_{r=0}^{\infty} \sum_{l,l'} {}_nC_r (M^r)_{il}(M^{n-r})_{jl'}A_{ll'}\,, \tag{A·4}$$

where M is a matrix whose i, j element is M_{ij}.

Then it can be readily verified that

$$\exp[t(1-\tilde{\mathcal{P}})\,(\tilde{H}_1+\tilde{H}_L)]\,A_{ij} = a_i(t)a_j(t) - \langle a_i(t)a_j(t)\rangle_l\,, \tag{A·5}$$

where

$$a_i(t) \equiv [\exp(tM)a]_i\,. \tag{A·6}$$

By inserting Eq. (A·5) to Eq. (16) we obtain

$$\langle A_{ij}\rangle_s = \int_0^\infty dt \langle O a_i(t) a_j(t)\rangle_l\,, \tag{A·7}$$

where we have made use of the fact that $\langle O\rangle_l = 0$.

Appendix B

An evaluation of the quantities (31) can be done in the same way as KG. We have briefly outline the procedure and give the results.

It can be easily shown that the quantities defined as

$$\begin{aligned}
\xi_1(\boldsymbol{k}) &\equiv \int_0^\infty dt\, \tfrac{1}{2}[u_{\boldsymbol{k}}{}^x(t)u^y_{-\boldsymbol{k}}(t) + u_{\boldsymbol{k}}{}^y(t)u^x_{-\boldsymbol{k}}(t)]\,,\\
\xi_2(\boldsymbol{k}) &\equiv \int_0^\infty dt\, u_{\boldsymbol{k}}{}^x(t)u^x_{-\boldsymbol{k}}(t)\,,\\
\xi_3(\boldsymbol{k}) &\equiv \int_0^\infty dt\, u_{\boldsymbol{k}}{}^y(t)u^y_{-\boldsymbol{k}}(t)\,,\\
\xi_4(\boldsymbol{k}) &\equiv \int_0^\infty dt\, u_{\boldsymbol{k}}{}^z(t)u^z_{-\boldsymbol{k}}(t)
\end{aligned} \tag{B·1}$$

satisfy the following differential equations:

$$\left(-2gk^2+k_y\frac{\partial}{\partial k_x}+\frac{4k_xk_y}{k^2}\right)\xi_2(\boldsymbol{k})=-\frac{1}{D}u_{\boldsymbol{k}}{}^x u^x_{-\boldsymbol{k}},$$

$$\left(-2gk^2+k_y\frac{\partial}{\partial k_x}+\frac{2k_xk_y}{k^2}\right)\xi_1(\boldsymbol{k})+\left(\frac{4k_y{}^2}{k^2}-1\right)\xi_2(\boldsymbol{k})=-\frac{1}{2D}(u_{\boldsymbol{k}}{}^x u^y_{-\boldsymbol{k}}+u_{\boldsymbol{k}}{}^y u^x_{-\boldsymbol{k}}),$$

$$\left(-2gk^2+k_y\frac{\partial}{\partial k_x}\right)\xi_3(\boldsymbol{k})+2\left(\frac{4k_y{}^2}{k^2}-1\right)\xi_1(\boldsymbol{k})=-\frac{1}{D}u_{\boldsymbol{k}}{}^y u^y_{-\boldsymbol{k}},$$

$$\xi_4(\boldsymbol{k})=\frac{1}{k_z{}^2}[k_x{}^2\xi_2(\boldsymbol{k})+k_y{}^2\xi_3(\boldsymbol{k})+2k_xk_y\xi_1(\boldsymbol{k})] \tag{B·2}$$

with

$$g\equiv\eta/(\rho D).$$

These equations are solved and yield

$$\xi_i(\boldsymbol{k})=-\int_{\infty\times Dk_y}^{k_x}dk_x'\frac{1}{Dk_y}K(\boldsymbol{k},\boldsymbol{k}')\Phi_i(\boldsymbol{k}'), \tag{B·3}$$

where

$$K(\boldsymbol{k},\boldsymbol{k}')\equiv\exp[(2g/k_y)\{k_x(k^2-2k_x{}^2/3)-k_x'(k'^2-2k_x'^2/3)\}] \tag{B·4}$$

and

$$\Phi_1(\boldsymbol{k}')=\frac{k'^2}{2k^2}(u^x_{\boldsymbol{k}'}u^y_{-\boldsymbol{k}'}+u^y_{\boldsymbol{k}'}u^x_{-\boldsymbol{k}'})-\frac{k'^4}{k_yk^2}F(k_x,k_x')u^x_{\boldsymbol{k}'}u^x_{-\boldsymbol{k}'},$$

$$\Phi_2(\boldsymbol{k}')=\frac{k'^4}{k^4}u^x_{\boldsymbol{k}'}u^x_{-\boldsymbol{k}'},$$

$$\Phi_3(\boldsymbol{k}')=u^y_{\boldsymbol{k}'}u^y_{-\boldsymbol{k}'}-\frac{k'^2}{k_y}F(k_x,k_x')(u^x_{\boldsymbol{k}'}u^y_{-\boldsymbol{k}'}+u^y_{\boldsymbol{k}'}u^x_{-\boldsymbol{k}'})+\frac{k'^4}{k_y{}^2}F^2(k_x,k_x')u^x_{\boldsymbol{k}'}u^x_{-\boldsymbol{k}'},$$

$$\Phi_4(\boldsymbol{k}')=u^z_{\boldsymbol{k}'}u^z_{-\boldsymbol{k}'}+\frac{k'^2}{k_z}G(k_x,k_x')(u^x_{\boldsymbol{k}'}u^z_{-\boldsymbol{k}'}+u^z_{\boldsymbol{k}'}u^x_{-\boldsymbol{k}'})+\frac{k'^4}{k_z{}^2}G^2(k_x,k_x')u^x_{\boldsymbol{k}'}u^x_{-\boldsymbol{k}'} \tag{B·5}$$

with

$$k'^2=k_x'^2+k_y{}^2+k_z{}^2$$

and

$$F(k_x,k_x')\equiv-\frac{k_z{}^2}{(k_y{}^2+k_z{}^2)^{3/2}}\tan^{-1}\left[k_y{}^2+k_z{}^2\frac{k_x-k_x'}{k_y{}^2+k_z{}^2+k_xk_x'}\right]+\frac{k_y{}^2(k_x-k_x')}{k^2k'^2}\left[1-\frac{k_xk_x'}{k_y{}^2+k_z{}^2}\right],$$

$$G(k_x,k_x')\equiv-\frac{k_z{}^2}{(k_y{}^2+k_z{}^2)^{3/2}}\tan^{-1}\left[k_y{}^2+k_z{}^2\frac{k_x-k_x'}{k_y{}^2+k_z{}^2+k_xk_x'}\right]-\frac{k_z{}^2(k_x-k_x')}{k^2k'^2}\left[1-\frac{k_xk_x'}{k_y{}^2+k_z{}^2}\right]. \tag{B·6}$$

Substituting Eq. (B·3) into Eq. (31) and using the relation

$$\langle u_{\boldsymbol{k}}{}^{\alpha} u^{\beta}_{-\boldsymbol{k}} \rangle_{l} = \delta_{\alpha\beta} - k_{\alpha}k_{\beta}/k^2, \quad (\alpha, \beta = x, y, z) \tag{B·7}$$

we obtain the following for the stress tensor:

$$\begin{aligned}
P^*_{xy} &= \frac{k_B T}{V} \sum_{\boldsymbol{k}} \int_{\infty \times Dk_y}^{k_x} dk_x' \frac{1}{k_y} K(\boldsymbol{k}, \boldsymbol{k}') \left[\frac{1}{k^2} \left(k_z^2 + \frac{2k_x'^2 k_y^2}{k'^2} \right) \right. \\
&\qquad \left. + \frac{2k'^2 k_x'}{k^2} \left(1 - \frac{k_x'^2}{k'^2} \right) F(k_x, k_x') \right], \\
P^*_{xx} &= - \frac{k_B T}{V} \sum_{\boldsymbol{k}} \int_{\infty \times Dk_y}^{k_x} dk_x' \frac{1}{k_y} K(\boldsymbol{k}, \boldsymbol{k}') \left(1 - \frac{k_x'^2}{k'^2} \right) \frac{k'^2 k_x' k_y}{k^4}, \\
P^*_{yy} &= - \frac{2k_B T}{V} \sum_{\boldsymbol{k}} \int_{\infty \times Dk_y}^{k_x} dk_x' \frac{1}{k_y} K(\boldsymbol{k}, \boldsymbol{k}') \left[\frac{k_x' k_y}{k'^2} \left(1 - \frac{k_y^2}{k'^2} \right) \right. \\
&\qquad \left. + \frac{1}{k_y} F(k_x, k_x') \left(k_z^2 + \frac{2k_x'^2 k_y^2}{k'^2} \right) + \frac{k'^2 k_x' k_y}{k_y^2} \left(1 - \frac{k_x'^2}{k'^2} \right) F^2(k_x, k_x') \right], \\
P^*_{zz} &= - \frac{2k_B T}{V} \sum_{\boldsymbol{k}} \int_{\infty \times Dk_y}^{k_x} dk_x' \frac{1}{k_y} K(\boldsymbol{k}, \boldsymbol{k}') \left[- \frac{k_z^2 k_x' k_y}{k'^4} + k_y \left(1 - \frac{2k_x'^2}{k'^2} \right) G(k_x, k_x') \right. \\
&\qquad \left. + \frac{k'^2 k_x' k_y}{k_z^2} \left(1 - \frac{k_x'^2}{k'^2} \right) G^2(k_x, k_x') \right].
\end{aligned} \tag{B·8}$$

Before proceeding further, the limiting values of these quantities for $D \to 0^+$ are examined and obtained as ($\nu \equiv \eta/\rho$)

$$\begin{aligned}
P^*_{xy} &\to - \frac{k_B T}{V} D \sum_{\boldsymbol{k}} \frac{1}{2\nu k^2} \left(\frac{k_z^2}{k^2} + \frac{2k_x^2 k_y^2}{k^4} \right), \\
P^*_{xx} &\to \frac{2k_B T}{V} D \sum_{\boldsymbol{k}} \frac{1}{2\nu k^2} \left(1 - \frac{k_x^2}{k^2} \right) \frac{k_x k_y}{k^2}, \\
P^*_{yy} &\to \frac{2k_B T}{V} D \sum_{\boldsymbol{k}} \frac{1}{2\nu k^2} \left(1 - \frac{k_y^2}{k^2} \right) \frac{k_x k_y}{k^2}, \\
P^*_{zz} &\to - \frac{2k_B T}{V} D \sum_{\boldsymbol{k}} \frac{1}{2\nu k^2} \frac{2k_z^2 k_x k_y}{k^4}.
\end{aligned} \tag{B·9}$$

The limiting values of the quantities P^*_{xx}, P^*_{yy} and P^*_{zz}, vanish due to symmetry. This result reflects the fact that these quantities are even function of D.[1] On the other hand P^*_{xy} in this limit does not vanish. By using the definition of the nonlinear shear viscosity, we obtain

$$\eta(0) = \frac{k_B T}{V} \sum_{\boldsymbol{k}} \frac{1}{2\nu k^2} \left(\frac{k_z^2}{k^2} + \frac{2k_x^2 k_y^2}{k^4} \right). \tag{B·10}$$

Equation (B·10) gives the linear part of the shear viscosity. By subtracting the linear part of the stress tensor from the nonlinear one, Eq. (B·8), the

remaining quantities are found to be convergent even if the upper limit of wave numbers k_M is taken to infinity and have the form const$\times k_BT(D/\nu)^{3/2}$. The constants C_i (see Eq. (34)) are numerically evaluated by the use of FACOM 230-60. The Simpson 1/3 rule is used for the numerical integration. The values are given in Eq. (34).

Appendix C

We consider the whole set of diagrams with $(2n)$ vertices, $n=1, 2, \cdots$, except for those containing self-energy corrections as in Fig. 3. Since we are interested in the order of magnitude of these diagrams with respect to k_0, propagators are simply classified into two species, an L- and a U-bonds: These propagators have internal momenta of order of k_0 and k_M, respectively. In Fig. 6 the dashed and the solid lines correspond to the L- and the U-bonds, respectively. Then, due to the momentum conservation law, only those vertices shown in Fig. 7 are allowed. Furthermore, either the dashed or the solid vertex shown in Fig. 8(A) [8(B)] appears in each diagram at the extreme left [right]. A part of a diagram not coming to pieces if L-bonds are removed is named "U-block" and indicated by a symbol U in the diagram. Here we give a rule to evaluate the order*) of a diagram. (A) An intermediate state containing only L-bonds (hereafter referred to as "L-state") gives the order k_0^{-2}. (B) Every vertex shown in Figs. 7(E)$\sim$(H) has a factor k_0, respectively. (C) In general, a $(2n)$-vertex diagram has $(n+1)$ independent integrals. If the integration variable is of $O(k_0)$, the order k_0^3 is given to the integral.

The following facts can be easily derived:

1) The decoration of a single L-bond by a U-block give the same order diagram as, or a higher order one than the original one (see Fig. 9).
2) The addition of a single L-bond to the original diagram yields a new diagram smaller than the original one at least by a factor k_0. This can be seen from

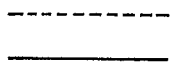

Fig. 6. U-bond and L-bond.

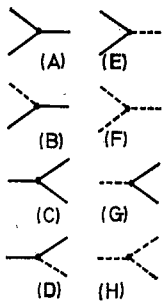

Fig. 7. Various types of bare vertices.

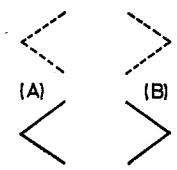

Fig. 8. Other types of vertices which appear at the extreme left and right of the diagram.

*) Hereafter by "order" we mean the "order of magnitude with respect to k_0" unless stated otherwise.

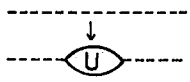

Fig. 9. Procedure (1).

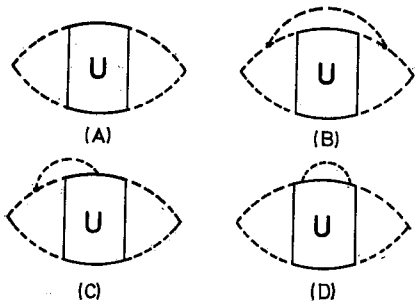

Fig. 10. Procedure (2).

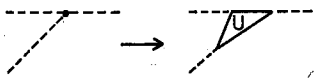

Fig. 11. Procedure (3).

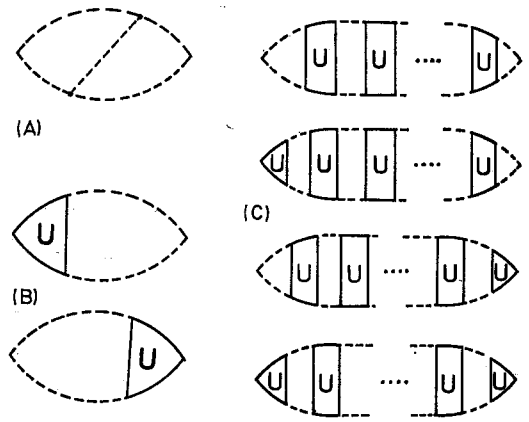

Fig. 12. The final set of diagrams which have to be considered.

an example in Fig. 10(B). Other examples shown in Figs. 10(C) and 10(D) are smaller than the original one by factors k_0^2 and k_0^3, respectively.

3) If the bare vertices, Figs. 7(F) and 7(H), are replaced by vertices of U-blocks, at least a factor of $O(k_0)$ is multiplied to the contribution of an original diagram, (see Fig. 11).

The whole diagram can be constructed of U-blocks, L-bonds and the dashed vertices in Figs. 7(F), 7(H) and 8. First we consider a diagram composed of a single U-block. Since the contribution from this diagram has a form const$+O(k_0^3)$, we may take no notice of this type of diagram as far as the lowest nonlinear correction is concerned. Next we consider a diagram whose intermediate states contain no L-state. The order of this diagram is at least k_0^3. Then we may also ignore this type of diagram. From now on we take account of the whole set of diagrams with $(2n)$ vertices $(n \geq 1)$ having at least one L-state; of course, this set does not contain a diagram of the type shown in Fig. 1 where the propagators are replaced by the renomalized ones. From this set we successively remove diagrams which can be obtained by the combination of procedures (1)$\sim$(3) as long as this manipulation does not yield the lowest order diagrams mentioned above. Finally we have a new set of diagrams from which we cannot take away any diagrams by the above-mentioned method. Diagrams in this set can be divided into two groups according to whether they contain U-blocks or not. The latter group consists of diagrams like one shown in Fig.

12(A). The order of these diagrams is k_0^2 which corresponds to Eq. (40). The former group consists of diagrams each of which has at most two L-bonds at every instant and have no vertices shown in Figs. 7(F) and 7(H), because otherwise we are always able to obtain a lower order than this by reversing procedures (1)$\sim$(3). If in a certain diagram of this group different U-blocks refer to the same time interval, this diagram can be omitted in our consideration since it is apparently of higher order than that shown in Fig. 12(B) or 12(C). Among the diagrams in Figs. 12(B) and 12(C), those in Fig. 12(B) give the lowest order contribution and their orders are at most k_0^2.

Finally we conclude that the lowest nonlinear correction to the stress tensor comes from the diagram in Fig. 1 with renormalized propagators. The resolvent operator formalism used in the present appendix is found in Ref. 2b) and the techniques developed in quantum many-body problem[10] can be used for this problem as well.

References

1) K. Kawasaki and J. D. Gunton, Phys. Rev. **A8** (1973), 2048.
2) a) K. Kawasaki, Ann. of Phys. **61** (1970), 1; in *Proceedings of the International Summer School of "Enrico Fermi", Varenna, Italy, 1970* (Academic Press, New York, 1971).
   b) R. Zwanzig, in *Proceedings of the Sixth IUPAP Conference on Statistical Mechanics*, eds. S. A. Rice et al. (The University of Chicago Press, Chicago and London, 1972).
3) K. Kawasaki, Prog. Theor. Phys. **51** (1974), 1064.
4) T. Yamada, Prog. Theor. Phys. **52** (1974), 1397.
5) T. Yamada and K. Kawasaki, Prog. Theor. Phys. **38** (1967), 1031.
6) V. M. Zaitsev and M. I. Shliomis, Soviet Phys.—JETP **32** (1971), 866.
7) M. Fixman and W. Botch, J. Chem. Phys. **36** (1962), 3100.
8) W. T. Ashurst and W. G. Hoover, Phys. Rev. Letters **31** (1973), 206.
9) H. Eyring et al., *Statistical Mechanics and Dynamics* (Wiley, New York, 1964).
10) Van Hove et al., *Quantum Theory of Many-Particle Systems* (W. A. Benjamin, New York, 1961).